◆ Human Brain Mapping 36:5168–5182 (2015) ◆

Phasic Stabilization of Motor Output After Auditory and Visual Distractors

Harri Piitulainen,[1†]* Mathieu Bourguignon,[1†] Eero Smeds,[1] Xavier De Tiège,[3] Veikko Jousmäki,[1,2] and Riitta Hari[1]

[1]*Brain Research Unit, Department of Neuroscience and Biomedical Engineering, Aalto University, AALTO, Espoo, Finland*
[2]*MEG Core and Advanced Magnetic Imaging (AMI) Centre, Aalto NeuroImaging, Aalto University, AALTO, Espoo, Finland*
[3]*Laboratoire De Cartographie Fonctionnelle Du Cerveau, UNI—ULB Neuroscience Institute, Université Libre De Bruxelles (ULB), Bruxelles, Belgium*

Abstract: To maintain steady motor output, distracting sensory stimuli need to be blocked. To study the effects of brief auditory and visual distractors on the human primary motor (M1) cortex, we monitored magnetoencephalographic (MEG) cortical rhythms, electromyogram (EMG) of finger flexors, and corticomuscular coherence (CMC) during right-hand pinch (force 5–7% of maximum) while 1-kHz tones and checkerboard patterns were presented for 100 ms once every 3.5–5 s. Twenty-one subjects (out of twenty-two) showed statistically significant ~20-Hz CMC. Both distractors elicited a covert startle-like response evident in changes of force and EMG (~50% of the background variation) but without any visible movement, followed by ~1-s enhancement of CMC (auditory on average by 75%, $P < 0.001$; visual by 33%, $P < 0.05$) and rolandic ~20-Hz rhythm (auditory by 14%, $P < 0.05$; visual by 11%, $P < 0.01$). Directional coupling of coherence from muscle to the M1 cortex (EMG→MEG) increased for ~0.5 s at the onset of the CMC enhancement, but only after auditory distractor (by 105%; $P < 0.05$), likely reflecting startle-related proprioceptive afference. The 20-Hz enhancements occurred in the left M1 cortex and were for the auditory stimuli preceded by an early suppression (by 7%, $P < 0.05$). Task-unrelated distractors modulated corticospinal coupling at ~20 Hz. We propose that the distractors triggered covert startle-like responses, resulting in proprioceptive afference to the cortex, and that they also transiently disengaged the subject's attention from the fine-motor task. As a result, the corticospinal output was readjusted to keep the contraction force stable. *Hum Brain Mapp 36:5168–5182, 2015.* © 2015 Wiley Periodicals, Inc.

Key words: magnetoencephalography; cortex–muscle coherence; sensorimotor integration; startle reflex; isometric contraction; sensorimotor cortex

[†]Harri Piitulainen and Mathieu Bourguignon equally contributed to the article.
The authors have no conflicts of interest to declare.
*Correspondence to: Harri Piitulainen, Brain Research Unit, Department of Neuroscience and Biomedical Engineering, Aalto University, PO Box 15100, 00076 AALTO, Espoo, Finland. E-mail: harri.piitulainen@aalto.fi

Received for publication 12 June 2015; Revised 11 September 2015; Accepted 14 September 2015.
DOI: 10.1002/hbm.23001
Published online 29 September 2015 in Wiley Online Library (wileyonlinelibrary.com).

© 2015 Wiley Periodicals, Inc.

INTRODUCTION

When at rest, the human primary sensorimotor cortex often exhibits a prominent "mu rhythm" that encompasses both alpha (~10 Hz) and beta (~20 Hz) frequencies as has been demonstrated in both electroencephalography (EEG; [Gastaut, 1952]) and magnetoencephalography (MEG; [Tiihonen et al., 1989]). The ~10 and ~20-Hz components of the mu rhythm are suppressed by active movements [Gastaut, 1952; Jasper and Penfield, 1949; Salmelin and Hari, 1994], passive movements [Alegre et al., 2002; Chatrian et al., 1959], and tactile stimulation [Chatrian et al., 1959; Cheyne et al., 2003; Salenius et al., 1997b]. The ~10 or ~20-Hz component of the mu rhythm can also be modulated by nonbiological visual stimuli [Vanni et al., 1999], spoken commands to move [Chatrian et al., 1959], action-related sounds [Caetano et al., 2007; Lepage et al., 2010], movement imagination [Pfurtscheller and Neuper, 1997; Schnitzler et al., 1997], and movement observation [Hari et al., 1998].

The coupling of the primary motor (M1) cortex to spinal α-motoneurons is reflected in the corticomuscular coherence (CMC): during sustained isometric contraction electromyographic (EMG) signals, representing motor unit firing, are coherent with MEG/EEG signals recorded from the M1 cortex [Brown et al., 1998; Conway et al., 1995; Gross et al., 2000; Halliday et al., 1998; Salenius et al., 1996,1997a]. The coherence peaks at about 20 Hz during low or intermediate contraction force. CMC is first phasically suppressed and then strongly enhanced after electrical median-nerve stimulation [Hari and Salenius, 1999; Tecchio et al. 2006b], and suppressed during ramp movements [Kilner et al., 1999], as well as after mechanical perturbation and electrical cutaneous stimulation [McClelland et al., 2012a]. CMC has thus been suggested to indicate a stabilized state of the M1 output [Kilner et al., 2000].

Visual stimulation has been shown to enhance EEG–EMG coherence [Safri et al., 2007, 2006]. Moreover, we have recently shown that MEG–EMG coherence is phasically increased during observation of another person's brief actions, at the same time as the M1 rhythms are suppressed at slightly lower frequencies, suggesting that different neurophysiological mechanisms are involved in the activation and stabilization of the M1 output during action observation [Hari et al., 2014]. Altogether, these results imply that both visual and somatosensory stimuli can affect brain rhythms in M1 cortex and the corticospinal coupling, with mechanisms depending on the stimulus type and context.

Uncovering the exact spatiotemporal dynamics of these CMC and mu rhythm modulations would bring novel insights into how external distractors, irrelevant to the motor task, affect M1 activity and motor output.

Here, we aimed to find out the effects of brief auditory and visual stimuli, irrelevant to the ongoing motor task, on M1-cortex activity during steady motor output. Our study was specifically designed to assess the spatiotemporal dynamics of stimulus-induced changes in the level of sensorimotor cortical rhythms as well as of corticospinal coupling as indexed by the CMC. Also, the spatiotemporal relationships between those changes were assessed in source space. The stimuli were presented at low but clearly perceivable intensity to avoid overt startle responses.

MATERIALS AND METHODS

Subjects

Twenty-two healthy volunteers (12 males, 10 females; age 19–38 years, mean 25.8 years) with no history of neuropsychiatric disease or movement disorders were studied. Twenty-one subjects were right-handed (mean score 88, range 58–100 on the scale from −100 to 100; Edinburgh handedness inventory [Oldfield, 1971] and one subject was ambidextrous (score 25).

The study had prior approval by the ethics committee of the Helsinki and Uusimaa Hospital District. The subjects gave informed consent before participation. Subjects were compensated monetarily for travel expenses and lost working hours.

Experimental Protocol

Before the MEG recordings, the maximum pinch-grip force between right thumb and index finger was measured with a rigid load cell (1042, Vishay Precision Group, Malvern, PA); the subjects performed two to three maximal contractions, each lasting 3–4 s, with 2-min rest periods in-between. Mean force over 1 s of stable contraction from the trial with the highest force level was considered the maximum voluntary-contraction (MVC) force.

Figure 1a illustrates the experimental setup. During MEG recordings, the subjects were sitting with their left hand on the thigh and their right hand on a table in front of them. When needed, the subject's vision was optically corrected with nonmagnetic goggles.

The subjects were asked to maintain a steady isometric pinch grip against flexible aluminum handles of another force transducer (Honeywell International, Morristown, NJ), positioned between the right thumb and the index finger and to fixate to a black cross (spanning 1.4 deg of visual angle) displayed on a grey background in the middle of a translucent screen. For the low-force task, we used a force transducer that was more sensitive than the one used to record MVC, thereby to maximize the resolution of the force recording. The subjects were also asked to follow auditory feedback that was presented whenever their force level stepped out of 5–7% of their maximum voluntary force, and accordingly readjust their force level. The feedback was a 500-Hz tone, delivered via a flat-panel speaker (Panphonics 60 × 60 SSHP, Tampere, Finland) on the wall of the magnetically shielded room, presented as long as the subject's force was outside the range. The

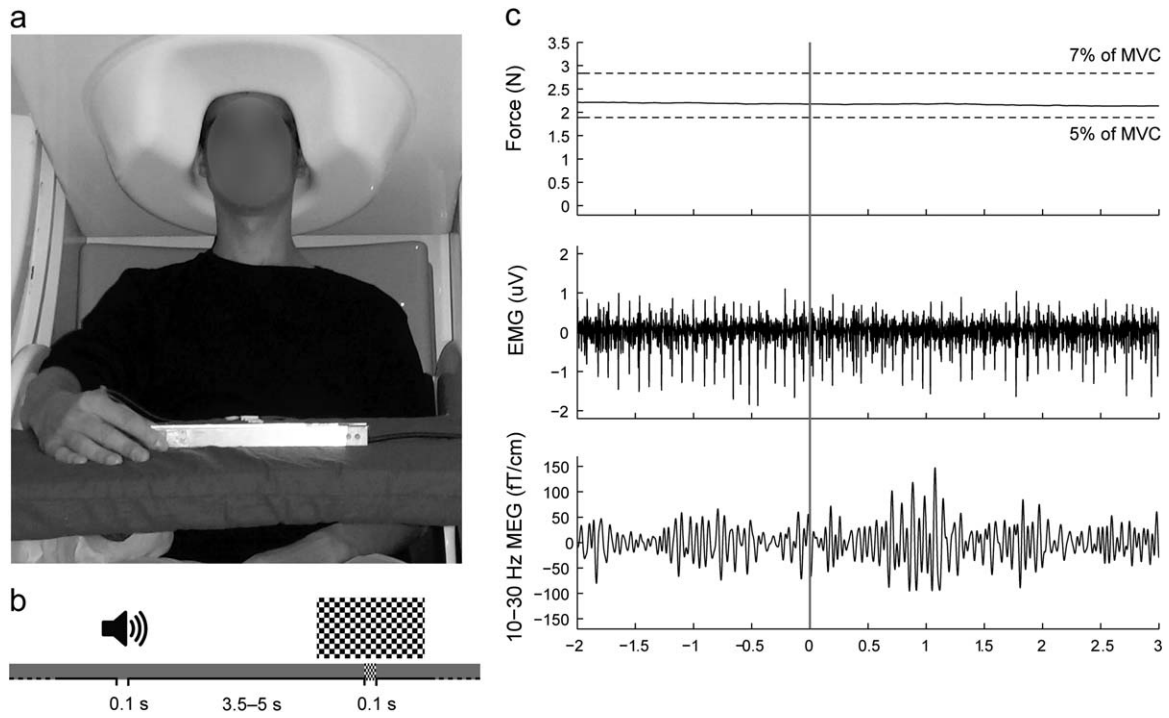

Figure 1.

Experimental setup and representative signals of subject S1. (**a**) Position of the subject during MEG recording. (**b**) Stimuli: auditory (binaural 1-kHz tones for 0.1 s) and visual (checkerboard pattern for 0.1 s) stimuli randomly presented every 3.5–5 s. (c) Examples of the measured signals as a function of time, shown for a 5-s epoch of isometric contraction. Rows from top to bottom: force (the horizontal dashed lines indicate the task limits, 5–7% of maximum voluntary contraction), wide-band EMG and 10–30-Hz MEG (from the channel showing the highest CMC). The grey vertical band indicates the occurence of auditory stimulus.

recordings were performed in four 5-min blocks, with a minimum of 2-min rest between the blocks. Subjects' brain activity at rest was recorded in separate 5-min sessions, while the subjects fixated to the same black cross as during the active conditions.

Figure 1b illustrates schematically the timing of the auditory and visual stimuli. Altogether 144 stimuli of both types were presented, in a random order once every 3.5–5 s (from onset to onset) in four recording blocks. The auditory stimuli (binaural 100-ms 1-kHz tones with 5-ms rise and fall times) were presented through plastic tubes and nonmagnetic earpieces directly into the ear canals (Etymotic Research, Elk Grove Village, IL), and they were easily discernible from the 500-Hz auditory feedback presented via the flat-panel speaker. Sound intensity was set to 60 dB above the individual hearing threshold, tested for both ears separately. The visual stimulus was a static black-and-white checkerboard pattern (14.6 deg × 8.2 deg, check size 0.7 deg × 0.7 deg) presented for 100 ms; the black fixation cross remained in the middle of the stimulus. Subjects were instructed to focus on maintaining the steady isometric contraction and to ignore the distractor stimuli.

Measurements

MEG

The MEG measurements were carried out in a magnetically shielded room (Imedco AG, Hägendorf, Switzerland) at the MEG Core of Aalto NeuroImaging, Aalto University, with a 306-channel whole-scalp neuromagnetometer (Elekta Neuromag^{TM}, Elekta Oy, Helsinki, Finland) that comprises 204 planar gradiometers and 102 magnetometers. The recording passband was 0.1–330 Hz and the signals were sampled at 1 kHz. The subject's head position inside the MEG helmet was continuously monitored by feeding current into four head-tracking coils located on the scalp; the locations of the coils and at least 200 head-surface points (scalp and nose) with respect to anatomical fiducials were determined with an electromagnetic tracker (Fastrak, Polhemus, Colchester, VT).

EMG and force

Surface EMG was measured from three synergistic finger flexor muscles of the right hand: first dorsal interosseus,

flexor digitorum superficialis, and flexor carpi radialis. EMG electrodes were placed in bipolar configuration (20-mm inter-electrode distance) over each muscle (impedance < 10 kΩ). Recording passband was 0.1–330 Hz. A force transducer with aluminum handles was used to measure the pinch force, and the signals were low-pass filtered at 330 Hz. Both EMG and force signals were sampled at 1 kHz and recorded time-locked to MEG signals.

MRI

The 3D-T1 magnetic resonance images (MRIs) were acquired with General Electric Signa® 3.0 T whole-body MRI scanner (Signa VH/i, General Electric, Milwaukee, WI) or with 3T MAGNETOM Skyra whole-body MRI scanner (Siemens Healthcare, Erlangen, Germany) at the AMI Center, Aalto NeuroImaging, Aalto University School of Science.

Data Processing

The analysis methods were adapted from Hari et al. [2014]. Analyses were performed with custom-made scripts in MATLAB 7.0 (MathWorks, Natick, MA) if not stated otherwise.

Preprocessing

Continuous MEG data were first preprocessed off-line using signal-space-separation (SSS; [Taulu et al., 2004]) to suppress external interferences and to correct for head movements. MEG (passband 1–195 Hz) and EMG (passband 5–195 Hz) were band-pass filtered offline and notch-filtered at 50 Hz and its harmonics. Force signal was low-pass filtered at 5 Hz.

Preliminary coherence analysis

In the preliminary coherence analysis, we estimated the CMC regardless of the distractors, in order to identify the optimal MEG sensor and muscle for further time-resolved analyses. Continuous data from the recording blocks were split into 1024-ms epochs with 819-ms epoch overlap [Bortel and Sovka, 2007], leading to frequency resolution of ~1 Hz. Epochs with MEG signals exceeding 6 pT (magnetometers) or 1.4 pT cm^{-1} (gradiometers) were rejected to avoid contamination of the data by artifacts in the MEG sensors. It is to be noted that eye movements and eye blinks produce artifacts at frequencies typically below 10 Hz and thus should not affect the CMC at ~20 Hz. Coherence spectra were computed between all MEG sensors and unrectified root-mean-square-normalized EMG signals following the formulation of Halliday et al. [1995], and by using multitaper approach (5 orthogonal Slepian tapers, yielding a spectral smoothing of ± 2.5 Hz) to estimated power- and cross-spectra [Thomson, 1982]. Then, for each subject and all three muscles, the gradiometer with the highest coherence peak in the 10–30-Hz band was selected among a predefined selection of 18 gradiometers (see Fig. 2a) covering the left rolandic region. We chose to use only gradiometers as they pick up cortical activity right underneath. The muscle and the corresponding gradiometer with the strongest coherence were used in further analyses. It is unlikely that this approach would bias the analysis as our interest was in event-related CMC modulations rather than in the absolute CMC levels. Moreover, synergistic muscles are known to receive common oscillatory synaptic inputs to their α-motoneurons, as is evident from coherent motor-unit firing at ~20 Hz [Farmer et al., 1993].

Effect of distractors on MEG–EMG coupling and power

We estimated the impact of the sensory distractors on the time–frequency dynamic of SM1 and muscle activity and their interplay. Trials were segmented from −2.5 s to 3.5 s relative to stimulus onsets. Artifact-free trials were analyzed when the coefficient of variation of the force (i.e., the ratio between its standard deviation and mean) was below an arbitrary threshold of 4%, indicating that the contraction remained steady. Power-, cross-, and coherence spectra were computed (at 0–45 Hz; with ±2.5 Hz spectral smoothing) between the selected MEG and EMG signals, using sliding 1,024-ms windows moved by 100-ms steps. This procedure yielded for each subject a time–frequency MEG and EMG power map, cross-spectral map, and coherence map with 51 time steps (from −2,000 ms to 3,000 ms by steps of 100 ms) and 47 frequency bins (from 0 to 45 Hz by steps of ~1 Hz). MEG and EMG power maps were further normalized by their mean baseline value (from −2,000 ms to −500 ms), separately for each frequency bin.

Renormalized partial directed coherence (rPDC; [Schelter et al., 2006, 2009]) was estimated between MEG and EMG signals, separately for each of the 1,024-ms windows described above. Estimating the rPDC requires fitting a multivariate autoregressive model to the data, and the parameters of the model determine the frequency resolution. The order of the model should be high enough to avoid spurious interactions and low enough for true interactions to survive the significance assessment [Schelter et al., 2009; Schneider and Neumaier, 2001; Sommerlade et al., 2009]. Because we aimed at evaluating the directional coupling for frequencies below 45 Hz, MEG and EMG signals were first low-pass filtered at 50 Hz and resampled at 100 Hz so that the ensuing 1020-ms epochs comprised 102 time bins. Then the ARfit package [Schneider and Neumaier, 2001] was used to fit a multivariate autoregressive model to the bivariate data constituted of the resampled MEG and EMG signals. Across subjects and conditions, the optimal model order (mean across the 51 time steps) according to the final prediction-error criterion [Akaike, 1974; Ding et al., 2000] was 56 ± 12 (mean ± SD; range: 22–78). Accordingly, a common model order of 50 was chosen, enabling us to evaluate the rPDC with fixed spectral resolution of 2 Hz for all subjects and conditions. Finally, to

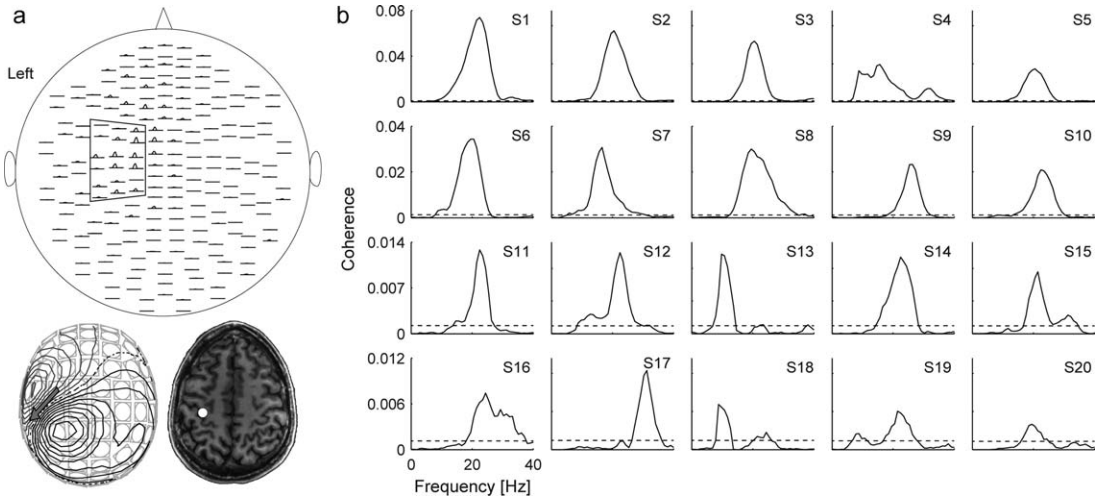

Figure 2.

Coherence spectra. (**a**) Spatial distribution of CMC spectra (pairs of orthogonal gradiometers are displayed; top), magnetic field pattern (bottom left) and the corresponding equivalent current dipole (ECD; bottom left and right) for a representative subject (S1) during isometric contraction. The ECD was estimated at the main peak (at 23 Hz) of the cross-spectrum, using a predefined subset of 18 planar gradiometers (surrounded on the left hemisphere) and a subject-specific spherical head model, and visualized on the subject's coregistered axial MRI (bottom right). Dipole analysis was performed with Neuromag® software suite. (**b**) Individual coherence spectra for 20 subjects; the signals are from the MEG sensor showing the strongest CMC. The dashed horizontal lines indicates threshold for statistical significance ($P < 0.05$).

achieve a frequency smoothing similar to that of power and coherence maps, rPDC was smoothed with a square kernel wide of 3 frequency bins, following the approach developed by [Sommerlade et al., 2009]. The ensuing spectral smoothing was ±3 Hz.

In summary, this procedure yielded for each subject and condition two time–frequency rPDC maps (MEG → EMG, and EMG → MEG) with 51 time steps (from −2,000 ms to 3,000 ms by steps of 100 ms) and 23 frequency bins (from 0 to 44 Hz by steps of 2 Hz). Group-level coherence, power, and rPDC maps were finally produced by averaging the maps across subjects.

Effect of distractors on muscle contraction

For each subject, force signals and rectified EMG signals were low-pass filtered at 5 Hz, normalized by their mean value, and averaged time-locked to stimulus onsets. The peak-to-peak amplitudes of these signals were compared, at individual and group level, with values obtained with surrogate data as described in Statistical analysis section below. To estimate the physiological relevance of these peak-to-peak values, we compared them with the background fluctuations estimated as the standard deviation (across time and epochs) of single-trial signals (low-passed at 5 Hz and normalized). Note that due to the normalization procedure, each trial had a mean equal to 1. Hence, the background fluctuations are directly expressed in percentage of the nominal force or EMG amplitude.

Effect of force variability on CMC modulation

We next tested the effect of force stability on CMC modulation. To do so, we computed the time–frequency dynamics of the CMC—as described in "Effect of distractors on MEG–EMG coupling and power" paragraph in Data processing section—separately for the most stable half of the trials (lowest coefficient of variation of the force) and for the most unstable half (highest coefficient of variation of the force still complying with the 4% limit fixed for accepting a trial).

Maps of source-level coherence and MEG power

Source reconstruction was performed to confirm the cortical origin of the group-level modulations disclosed by the sensor analyses. To that aim, individual MRIs were first segmented using Freesurfer software (Martinos Center for Biomedical Imaging, Charlestown, MA). MEG and segmented MRI coordinate systems were co-registered using the three anatomical fiducial points for initial estimation and the head-surface points to manually refine the surface co-registration. Then, the MEG forward model based on a one-shell boundary element model of individuals' intracranial space was computed for the three orthogonal current dipoles placed on a homogeneous 5-mm-grid source space that covered the whole brain (MNE suite; Martinos Center for Biomedical Imaging, Charlestown, MA).

For each source, the forward model was then reduced to its two principal components of highest singular value,

which closely correspond to sources tangential to the skull. Individual coherence and power maps were then produced within the computed source space at frequencies matching the statistically significant sensor-level effects, and at timings as in the sensor-level analysis (51 time-windows, from −2,000 ms to 3,000 ms by steps of 100 ms). Power maps were normalized similarly as at sensor-level, with a baseline from −2,000 ms to −500 ms. Projection in the source space was performed with Dynamic Imaging of Coherent Sources (DICS), with a regularization parameter equal to 1% of the maximum eigenvalue of the cross-spectral density matrix [Bourguignon et al., 2012a,b; Gross et al., 2001]. Data from planar gradiometers and magnetometers were simultaneously used for source estimation. To do so, sensor signals (and the corresponding forward-model coefficients) were normalized by their noise root-mean-square prior to computing DICS beamformer. The noise root-mean-square was estimated from the wide-band (1–195-Hz) continuous MEG signals at rest. Then, a non-linear transformation from individual MRIs to the standard Montreal Neurological Institute (MNI) brain was computed using the spatial-normalization algorithm implemented in Statistical Parametric Mapping (SPM8; Wellcome Department of Cognitive Neurology, London, UK; [Ashburner et al., 1997; Ashburner and Friston, 1999]) and applied to individual maps. Finally, group-level maps were obtained by averaging normalized maps across subjects.

Statistical Analysis

Preliminary coherence analysis

We used surrogate-data-based statistics to assess the statistical significance of coherence level in the 10–30-Hz frequency range, separately for each subject. This statistical procedure intrinsically corrects for multiple comparisons across sensors and frequencies. For each subject and condition, 1,000 surrogate coherence spectra were obtained by computing coherence between real MEG signals and Fourier-transform surrogate EMG signals. The Fourier-transform surrogate imposes power spectrum to remain the same as in the original signal but it replaces the phase of Fourier coefficients by random numbers in the range $(-\pi; \pi)$ [Faes et al., 2004]. Then, a single maximum coherence value across the preselected 18 gradiometers in the 10–30-Hz frequency range was extracted for each surrogate coherence spectrum. Finally, the 95-percentile of these values yielded the coherence threshold at $P < 0.05$ corrected for multiple comparisons across sensors and frequencies.

Effect of distractors on MEG–EMG coupling and power

The statistical significance of stimulus-induced modulation in time-frequency maps was tested for by comparing them with maps obtained with original MEG and EMG signals while replacing the stimulus onsets with dummy onset-series. The first dummy onset was randomly chosen in a 3-s interval centered on the first stimulus onset; the remaining dummy onset-series was constructed from the randomly shuffled times between all consecutive stimulus onsets. Such dummy data have the same properties as the original data (power spectra, coherence spectra), but they are not linked to the original stimulus onsets. For all subjects, 1,000 dummy power-, cross-spectral, coherence, and rPDC time-frequency maps, as well as averaged force and rectified EMG signals were computed—as described in "Effect of distractors on MEG–EMG coupling and power" paragraph of Data processing section—with 1,000 different dummy onset-series, and averaged across subjects to obtain 1,000 group-level dummy data sets. Dummy coherence maps were used to detect clusters of adjacent resels (resolution elements, i.e. the equivalent in time-frequency maps of pixels in normal images) of increased or decreased coherence from the corresponding map. First, a threshold indicating a statistically significant increase (decrease, respectively) in group-level coherence was computed for each resel as the 95-percentile (5-percentile, respectively) of the dummy coherence value in this resel. Then, clusters of group-level coherence above (below, respectively) the resel-specific threshold were extracted. Finally, to assess the statistical significance of these clusters, the same clustering analysis was performed with the group-level dummy coherence maps to extract the 97.5-percentile of the maximum cluster-size (as measured by the number of resels it contains). A cluster larger than the 97.5-percentile corresponds to a statistically significant increase or decrease of coherence at $P < 0.05$ (Bonferroni corrected for the two comparisons). The normalized MEG and EMG power maps and rPDC maps (in both directions) were assessed in a similar manner.

Effect of distractors on muscle contraction

Surrogate force and rectified EMG signals were used to assess the stability of stimulus-related force and EMG signals. Briefly, the largest variations of the force and rectified EMG signals were compared with the distribution obtained with the surrogate signals.

Effect of force variability on CMC modulation

The effect of stable vs. unstable force on CMC modulation was quantified with the differences (between data for stable vs. unstable force) in mean CMC values within clusters identified in preceding analyses. The statistical significances of these differences were assessed by comparing them with their distributions when the trials were randomly split into two halves (1,000 repetitions).

RESULTS

Figure 1c illustrates for a representative subject (S1) force, EMG, and MEG signals during 5 s of the isometric pinch

grip. No changes are visible in association with the auditory distractor occuring at time 0. Altogether 21 subjects (out of 22) were able to maintain the isometric force within the task limits throughout the measurement blocks, and 20 of them displayed statistically significant ($P < 0.05$) coherence between MEG and EMG signals at least for one of the three studied muscles. Thus, the following results include data from 20 subjects, including the ambidextrous subject.

Preliminary Coherence Analysis

Figure 2a shows the spatial distribution of the CMC spectra for one representative subject (S1; same as in Fig. 1) during isometric contraction. The spectra peaked at 23 Hz and the corresponding magnetic field pattern of the cross-spectrum (bottom left panel) was nicely dipolar, with an equivalent current dipole located in the hand knob of the M1 cortex (bottom right panel), in agreement with earlier studies [Salenius et al., 1997a].

Figure 2b shows for all 20 subjects the individual CMC spectra computed from 6,400 to 6,940 epochs; on average 1.5% (range 1.2–2.4%) of the epochs were rejected from this coherence analysis. The coherence peaked at 20.5 ± 1.0 Hz (mean ± SEM; range 11–29 Hz). For each subject, the muscle yielding the highest CMC was selected for further analysis (the first dorsal interosseus for six subjects, the flexor digitorum superficialis for nine subjects, and the flexor carpi radialis for five subjects).

Effect of Distractors on Muscle Contraction

Figure 3a presents the normalized force and Figure 3b the EMG signals for all individuals time-locked to onsets of auditory (left panels) and visual (right panels) distractors. From the 144 epochs, on average 9.0% (range 0.7–32.6%) were rejected for the auditory and 10.4% (range 0.7–41%) for the visual distractors because of artifacts or unstable contraction force. On average, the subjects corrected their force 32.3 ± 21.0 (mean ± SD; range 10–91) times during the 20-min recording.

A covert startle-like response, below the level of normal background fluctuation of the isometric contraction, was detected in the force and EMG signals. At the group level (thick black lines), both the force and the EMG showed subtle but statistically significant changes (with respect to mean values), starting ~30–50 ms after the presentation of the distractors ($P < 0.001$ for all). These changes were statistically significant ($P < 0.05$) in most subjects for the auditory distractors (8/20 subjects for force; 13/20 for EMG), but only in few subjects for the visual distractors (3/20 subjects for force; 3/20 for EMG). However, the mean peak-to-peak changes were only about half of the background fluctuations: $47\% \pm 15\%$ (range 29%–82%) force and $56\% \pm 14\%$ (35%–87%) EMG changes for auditory distractors, and $37\% \pm 18\%$ (13%–77%) force and $42\% \pm 6\%$ (22%–52%) EMG changes for visual distractors. The background force variation itself was only ~1% of the nominal force ($1.2\% \pm 0.4\%$, range 0.7%–2.0% for auditory, and $1.1\% \pm 0.4\%$, range 0.6–1.9% for visual distractros), and the background EMG variation was ~15% of the mean EMG amplitude ($15\% \pm 2\%$, range 12%–21% for auditory, and $15\% \pm 3\%$, range 12%–22% for visual distractors).

Effect of Distractors on MEG–EMG Coupling and Power

Figures 3c,d present group-level stimulus-related time-frequency CMC and MEG power maps computed from subject-specific single gradiometers that showed the peak coherence in the left sensorimotor hand region. Figure 3e shows the respective time-frequency EMG-power maps. Please note that values at a given time in power and coherence maps are obtained from signals in 1-s windows centered on that time (i.e. ±0.5 s around the indicated time). For this reason, modulation in coherence and power are visible before the stimulus onset. For example, in the auditory-stimulus-related power map the very abrupt < 10-Hz power change at −300 ms (analysis window from −811 ms to 212 ms) reflects the 100-ms auditory evoked response that was picked up to some extent by the selected rolandic sensors. The distinction between auditory-cortex and rolandic contributions to CMC and power modulations is discussed in more detail in association of the spatial maps (see Fig. 4 and the related text below).

Table I lists statistically significant modulations of CMC, MEG, and EMG power to the distractors. The auditory distractors (Fig. 3c,d, left column) elicited simultaneous enhancements of CMC (by 75%; $P < 0.001$) and MEG power (14%; $P = 0.03$), and early suppression of MEG power (8%; $P = 0.037$). In addition, enhancement of EMG power (8% at 21 Hz; $P < 0.001$) was detected, and this cluster showed also a distinct earlier enhancement of EMG power (6% at 13 Hz). The visual distractors (Fig. 3c,d, right column) enhanced CMC (33%; $P = 0.002$) and MEG power (11% at 21 Hz, $P = 0.011$; 5% at 33 Hz, $P = 0.038$). The EMG power was also enhanced (by 7%; $P = 0.01$) after presentation of the visual distractor.

Figure 3f compares directly the 10–30-Hz CMC (solid lines) and MEG power (dashed lines) as a function of time, emphasizing the similarity of their time courses.

Maps of Source-level Coherence and MEG Power

Figure 4 shows the temporal evolution of group-level CMC at 20 Hz and MEG power at 20 and 8 Hz, separately for auditory and visual distractors (upper and lower panels, respectively). Increased CMC was well co-localized with the ~20-Hz MEG power modulations (enhancement after both distractors and early suppression after auditory distractors) in the subjects' right-hand region of the left M1 cortex. Modality-specific auditory and visual evoked responses were visible in 8-Hz MEG power modulations

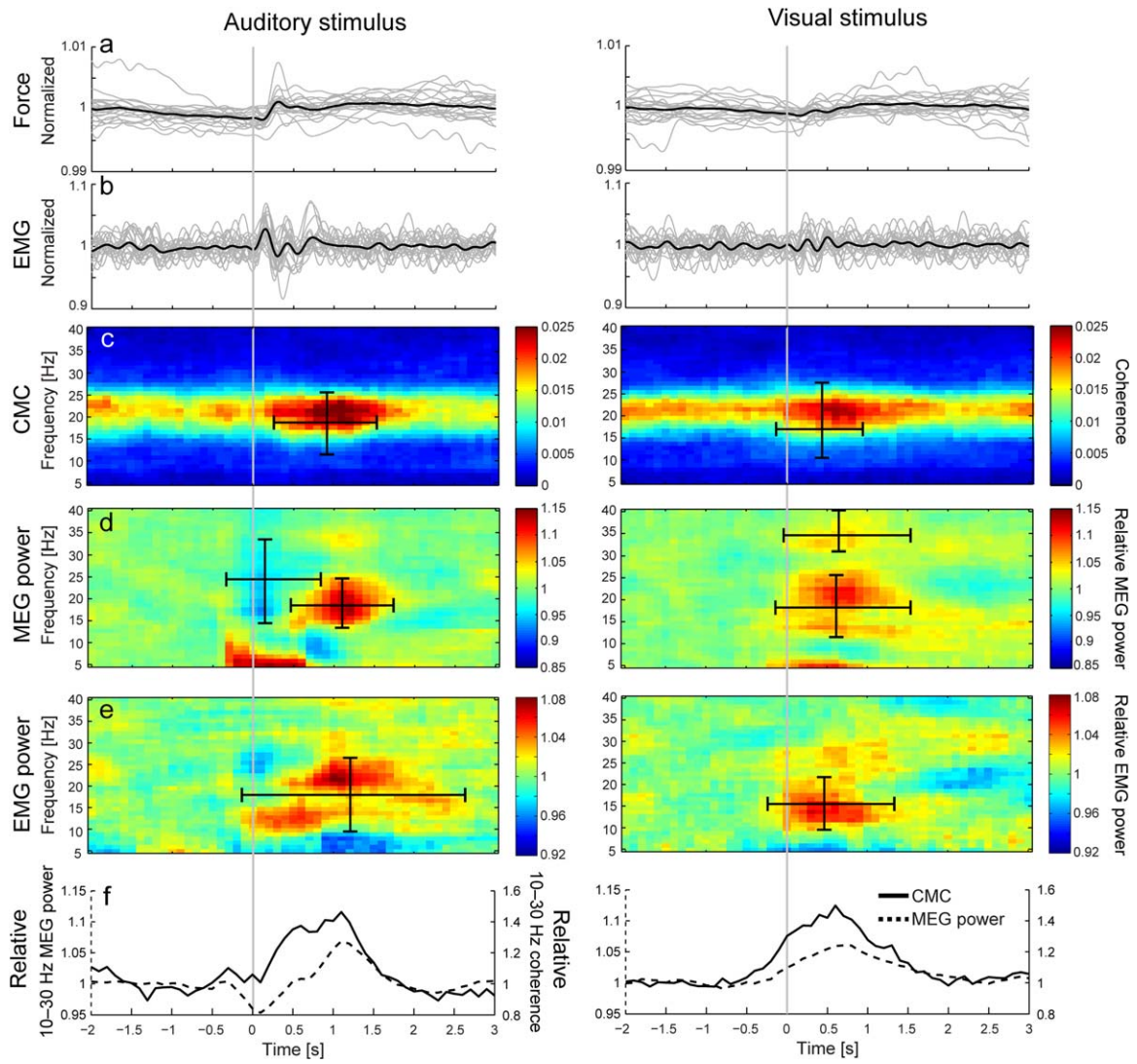

Figure 3.

Results of the stimulus-related analysis for 20 subjects. (**a** and **b**) Normalized group-level (black line) and individual (grey lines) force (a) and EMG (b) values low-pass filtered at 5 Hz. (**c**–**e**) Group-level time-frequency CMC (c), MEG power (d) and EMG power maps (e). (**f**) Relative modulations of 10–30-Hz CMC (solid line) and MEG power (dashed line). The CMC and MEG power maps were computed for a single gradiometer that showed the strongest coherence in the subject's left M1 cortex (corresponding to right hand). Ranges of statistically significant enhancements and suppressions are indicated with horizontal (time) and vertical (frequency) bars superimposed on the map (c–e). All maps and values are time-locked to the onset of auditory (1st column) or visual (2nd column) distractors, indicated by the grey vertical lines. The stimulus-related force and EMG traces were normalized by their mean values. Please note that due to the method used to compute coherence and power, values at a given time-point reflect signals ± 0.5 s around. For this reason, modulation in coherence and power are already visible before the stimulus onset.

at temporal and occipital areas, respectively. Note that statistics were performed at sensor and not source level.

Directional Coupling Between MEG and EMG

Figure 5 shows the temporal evolution of the directional coupling from MEG to EMG and *vice versa*. The directional coupling was globally stronger from the M1 cortex to the muscle (MEG → EMG), however, only the directional coupling from muscle to the M1 cortex (EMG → MEG) increased phasically after auditory distractor (by 105%; $P = 0.011$; peaking at 22 Hz and 400 ms; cluster size 27; frequency range 10–22 Hz and time range 300–900 ms). This increase coincided with the onset of the CMC enhancement,

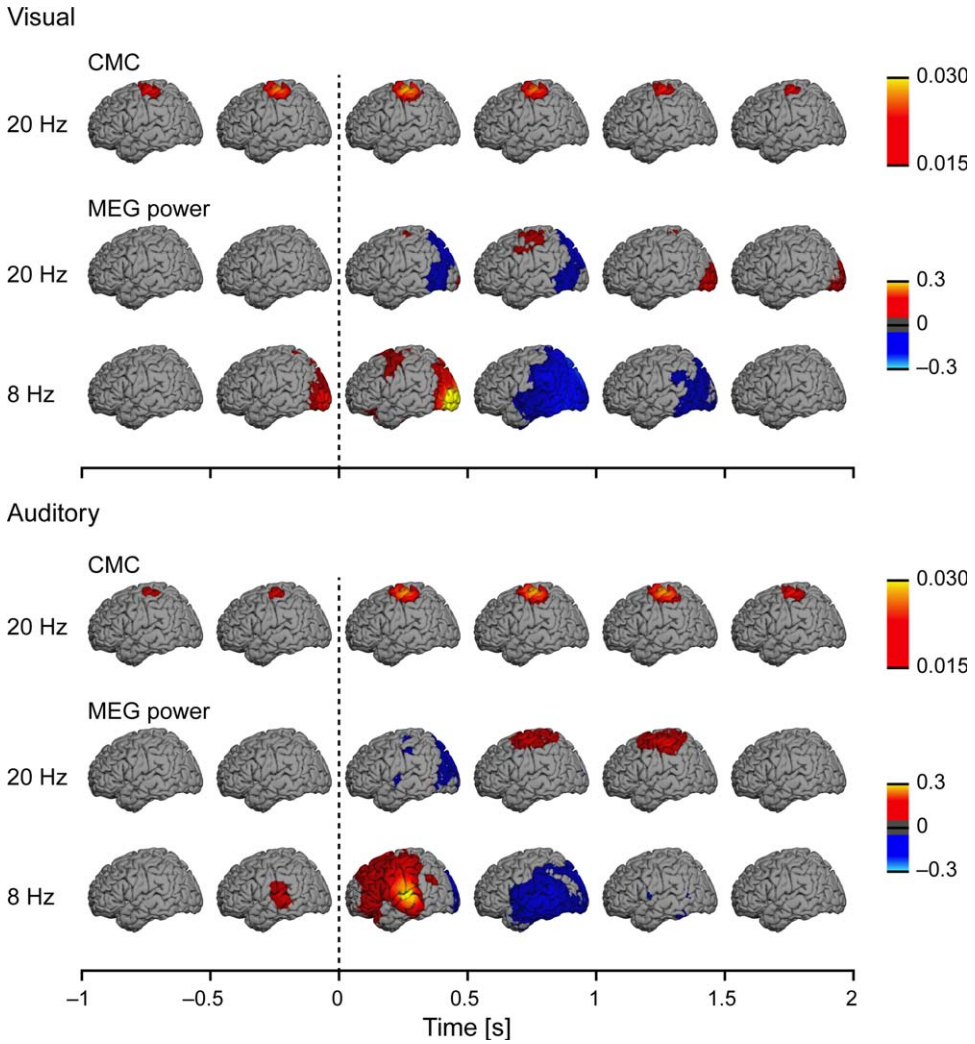

Figure 4.

Source reconstructions at the group level ($n = 20$) separately for the coherence at the frequency bin corresponding to 19.5 Hz (first row) and for the relative MEG power at 19.5 and 7.8 Hz (second and third row). Each map was computed as the mean coherence/power across time-bins spanning the 0.5-s time window above which it is centered on (e.g., maps displayed above the 0–0.5-s time-window reflect the mean of the 6 maps computed at 0, 0.1, 0.2, 0.3, 0.4, 0.5 s). Other details as in Figure 3.

but it returned to baseline earlier than the CMC. No other increase or decrease reached statistical significance in either of the directions and for either of the distractors.

Effect of Force Variability on CMC Modulation

Figure 6 shows the CMC time–frequency maps computed separately based on trials with the most stable and most unstable force. For the auditory distractors, the mean CMC within the cluster identified above (cluster of increased CMC) was statistically significantly higher ($P = 0.006$) when evaluated from trials with unstable force compared with stable force. The mean CMC enhancement induced by auditory distractors was of 123% during unstable force and of 23% during stable force. The inspection of the force traces revealed that the main difference was an enhanced early-onset increase in force level for unstable trials. For visual distractors, the CMC modulation did not differ for trials with stable or unstable force ($P = 0.33$).

DISCUSSION

We found that ~20-Hz corticospinal coupling, represented by the strength of CMC, and the MEG power were transiently enhanced by task-irrelevant brief auditory and visual

TABLE I. Significant modulations of CMC, MEG power, and EMG power by the distractors

	Auditory			Visual		
	Peak (range) frequency (Hz)	Peak (range) latency (s)	Change	Peak (range) frequency (Hz)	Peak (range) latency (s)	Change
CMC	21 (12–25)	1.1 (0.3–1.5)	+	21 (11–27)	0.6 (−0.1–0.9)	+
MEG power	18 (15–33)	0.1 (−0.3–0.8)	–	33 (31–39)	0.4 (0–1.5)	+
	19 (14–24)	1.2 (0.5–1.7)	+	22 (12–25)	0.8 (0.1–1.5)	+
EMG power	21 (10–26)	1.1 (−0.1–2.6)	+	14 (10–21)	0.3 (−0.2–1.3)	+

In Change, + refers to increase and – to decrease of coherence or power.

stimuli (distractors) during steady isometric contraction. These increases were preceded by a subtle increase in muscle output (a covert startle-like response), which was followed by enhancement of directional coupling from muscle to M1 cortex within the same ~20-Hz frequency band (statistically significant only for auditory distractors). On the basis of source analysis, and in agreement with our previous studies [Salenius et al., 1997a; Salmelin and Hari, 1994; Salmelin et al., 1995], both the CMC and the ~20-Hz rhythm originated from the M1 cortex contralateral to the contracted muscles. For auditory distractors, the enhancements were preceded by an early suppression of ~20-Hz rhythm (peaking at ~0.1 s). Altogether our results suggest that the M1 cortex was inhibited, reflecting suppression (either in the motor cortex or elsewhere) of the effects of the auditory and visual distractors to maintain stable M1 output.

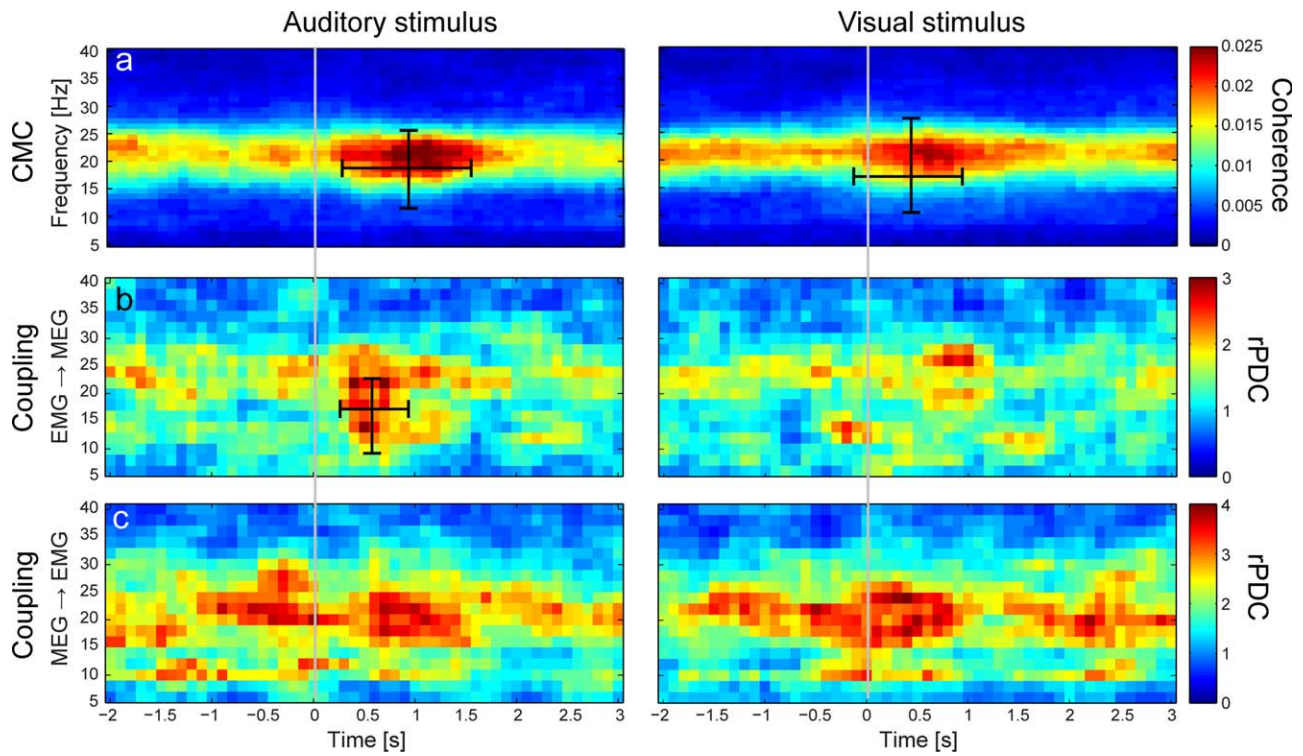

Figure 5.

Group-level ($n = 20$) time-frequency CMC (**a**), and directional coupling maps (**b**: EMG → MEG; **c**: MEG → EMG). Values of directional coupling (rPDC: renormalized partial directed coherence) are normalized so that individual values follow a Chi square distribution with 2 degrees of freedom. All maps and values are time-locked to the onset of auditory (1st column) or visual (2nd column) distractors, indicated by the grey vertical lines. Ranges of statistically significant enhancements and suppressions are indicated with horizontal (time) and vertical (frequency) bars on the maps. Please note that values at a given time point reflect signals from a 1-s time window centered on that point.

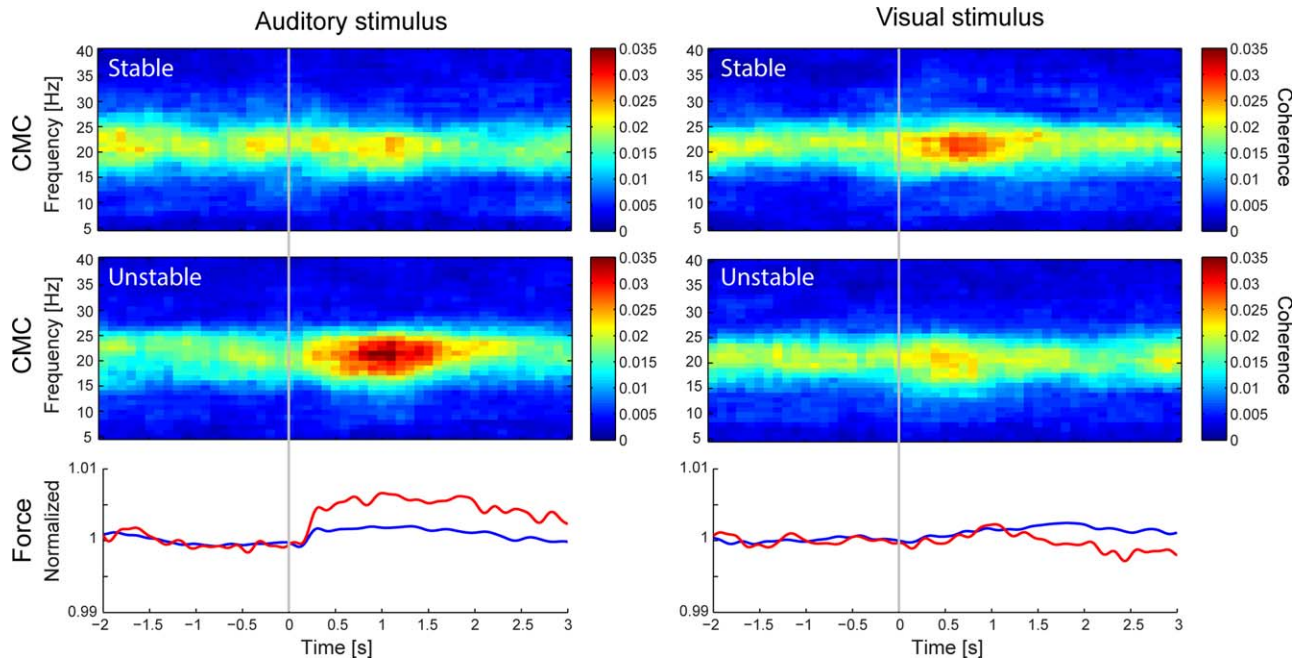

Figure 6.

Group-level ($n = 20$) time-frequency CMC maps computed separately for the stable (upper row) and unstable force (middle row) half of the trials. The respective mean force is shown in blue for stable half of the trials and in red for the unstable ones (bottom row). All maps and values are time-locked to the onset of auditory (1st column) or visual (2nd column) distractors, indicated by the grey vertical lines.

Auditory–Distractor-related Modulations

To our knowledge, ours is the first study to show that pure tones can enhance CMC in a way that resembles the effect of visual stimuli. Some prior evidence exists about the reactivity of the mu rhythm to sounds. The rolandic 10-Hz EEG rhythm is blocked shortly (~0.35 s) after the onset of a heard verbal command to move, irrespective of the duration of the command [Chatrian et al., 1959]. Motor-action-related sounds modulate the both the ~10- and ~20-Hz components of the rolandic mu rhythm (drum-tapping during MEG, [Caetano et al., 2007]; finger-clicks during intracranial EEG, [Lepage et al., 2010]), whereas pure tones have been ineffective in modulating both MEG [Caetano et al., 2007] and EEG [Crawcour et al., 2009] mu rhythms. One reason why pure tones affected the mu rhythm in our study might be that our subjects were studied while they were engaged in a skill- and stability-demanding motor task.

Visual–Distractor-related Modulations

The observed CMC enhancement by visual distractors agrees with previous EEG experiments, in which ~15–25-Hz EEG–EMG coherence was enhanced during repetitive visual stimuli [Safri et al., 2007, 2006]. However, in contrast to our results, those EEG studies did not find modulation of the mu rhythm (13–30 Hz), possibly because the short 1-s inter-stimulus-interval they used. After somatosensory stimuli, the strength of CMC covaries with the rolandic ~20-Hz MEG power [Hari and Salenius, 1999], suggesting that CMC and ~20-Hz MEG power are related to similar changes in the functional state of the M1 cortex. The current co-variation of CMC and rolandic ~20-Hz MEG power roughly agrees with this view.

Modulation of the mu rhythm by visual and auditory stimuli has also been studied in subjects who are not simultaneously performing any motor actions. For example, during binocular rivalry, sudden drifting of a visual grating enhanced the MEG mu rhythm at 8–15 Hz, starting ~0.45 s after stimulus onset [Vanni et al., 1999], indicating that visual information can modulate mu rhythm even in subjects not engaged in motor tasks. Our observations further indicate that visual distractors can affect corticospinal coupling during motor action, eliciting physiological changes that may be interpreted as covert startle responses. Although the effects appeared weaker than for the auditory distractors, any comparisons between the stimuli of these two senses are not justifiable here as the stimulus intensities were not matched.

Active Stabilization of the M1 Output

CMC is typically enhanced immediately after transition from phasic to steady contraction, meaning that the enhancement of CMC could reflect stabilization and/or recalibration of the M1 output [Baker, 2007; Kilner et al., 2000]. Accordingly, the enhancement of ~20-Hz mu rhythm has been suggested to reflect increased inhibition in the M1 cortex [Gastaut, 1952; Salmelin et al., 1995] and to promote the existing motor and postural state [Gilbertson et al., 2005]. In other words, the ~20-Hz mu-rhythm enhancement could be related to stabilization of the motor output (for a review, see [Engel and Fries, 2010]). In response to median nerve stimulation, enhancement (i.e., rebound) of ~20-Hz mu rhythm occurs typically between ~0.2 and 1 s [Salenius et al., 1997b; Salmelin and Hari, 1994], which a later transcranial magnetic stimulation study showed to coincide with reduced M1-cortex excitability [Chen et al., 1999].

In the current study, the randomly presented visual and auditory stimuli served as distractors unrelated to the fine-motor task and the subjects were instructed to ignore them. However, any change in the sensory environment may affect the motor control and M1 activity via reciprocal sensorimotor connections involving premotor and parietal regions [Rizzolatti et al., 1998]. The fMRI signals of both superior parietal and premotor cortices are increased when irrelevant visual distractors are presented during a visual-search task [de Fockert et al., 2004], and the appearance of behaviorally irrelevant visual distractors during a stop-signal task activates a very similar extensive brain network as does the actual stopping [Sharp et al., 2010]. Thus the ability to inhibit distractors seems critical for the maintenance of the ongoing motor action. Other brain areas that might be involved include the basal ganglia that are important for inhibiting ongoing motor action [Aron and Poldrack, 2006; Kühn et al., 2004; Ray et al., 2012].

We thus conjecture that steady M1 output can be maintained only when the effects of external distractions are actively blocked. The phasic enhancements of the rolandic ~20-Hz MEG power and CMC (in good spatial, temporal and spectral alignment) could reflect such M1 inhibition and stabilization, necessary for stable corticospinal output.

Startle-like Responses Elicited by the Distractors

In all subjects, both distractors elicited minute, but significant, stimulus-locked EMG increases and modulation of the isometric force by <0.02 N, which is, however, only a fiftieth of the task limits and half of the ~1% background variability of the force. These subtle modulations of the applied force unlikely reflect phasic changes in M1 output, as the short (~30–50 ms) latency of the EMG-modulation onset suggests involvement of a reflexive pathway—such as a covert startle-like response (see below). Nevertheless, the phasic increase of the directional coupling from periphery to the M1 cortex (EMG → MEG) during the initial phase of the CMC enhancement suggests that this subtle motor response activated proprioceptive afferents. However, the increase in directional coupling was statistically significant only for the auditory distractors. Interestingly, the stronger motor response (and thus stronger proprioceptive afference) was associated with stronger CMC modulation, but again only for auditory distractors (see Fig. 6).

Sudden loud sounds can elicit a short-latency acoustic startle reflex (or orientation reaction) that involves activation of hundreds of α-motoneurons along the length of the spinal cord (for a review, see [Yeomans and Frankland, 1995]). Although we did not observe any signs of overt startle reflexes, even nonstartling sounds can facilitate the spinal α-motoneuron pool, as indicated by the increased amplitude of the tibial H-reflex, starting 50–60 ms after sound onset and lasting for 200–250 ms [Rossignol and Jones, 1976]. Such spinal facilitation, possibly via the fast descending reticulospinal pathway [Davis et al., 1982], which is known to monosynaptically excite α-motoneurons of hand muscles [Riddle et al., 2009], could in part explain the subtle increases of EMG and force after the auditory distractors. In humans, a similar startle mechaniss has not been demonstrated for visual stimuli, which in the present study elicited weaker but otherwise rather similar peripheral effects, but only the auditory distractors were associated with an early suppression of the rolandic ~20-Hz MEG power (note that the stimulus intensities were not matched cross-modally).

The covert startle-like response and the concomitant proprioceptive afference could in part explain the decrease of the rolandic MEG power immediately after the onset of the auditory distractor. It is also possible that the distractor-locked proprioceptive afference could contribute to the enhancement of CMC ~1 s later because activation of proprioceptive afferents by hand movements or median-nerve stimulation elicits, after the early suppression, a rebound both in MEG power and CMC level [Kilner et al., 1999; Hari and Salenius, 1999]. However, some additional mechanisms seem necessary to explain all effects of the two distractors.

Disengagement of Attention by the Distractors

Changes in subject's attention could in part explain our observations, as dividing attention between motor and arithmetic tasks has been shown to affect the level of EEG–EMG coherence [Kristeva-Feige et al., 2002; Safri et al., 2007]. A plausible explanation for the observed effects is that the distractors caused a transient and weak bottom-up disengagement of the subject's attention from the motor task, meaning that the involvement of the sensorimotor cortex transiently decreased while auditory or visual cortices were needed for processing of the distractors. This interpretation would be in line with earlier EEG findings showing that the level of rolandic mu rhythms is

enhanced during a visual task and that the posterior alpha is increased during a motor task (e.g., [Pfurtscheller, 1992]). These effects would not necessitate direct access of auditory or visual stimuli to the M1 cortex to modulate the mu-rhythm level; rather a switch between dominant sensory modalities could happen at e.g. thalamic level, via mechanisms that remain speculative at present. Still startle could explain the early reduction of the ~20-Hz mu rhythm shortly after auditory but not visual stimuli.

Effects of MEG and EMG Amplitude Modulations on CMC

Both auditory and visual distractors enhanced EMG and rolandic MEG power with time courses coinciding with the enhancement of the ~20-Hz CMC. Previous research has shown that during isometric contraction the ~20-Hz power of EMG, the 20-Hz power of rolandic MEG and the synchronization index between these two signals covary with slow time courses of the order of tens of seconds [Gross et al., 2000]. In other words, the level of the motor-cortex control of muscle contraction in general covaries with MEG power. However, the effect of signal-to-noise ratio (SNR) also has to be considered as, in noisy signals, the synchronization may increase with improved SNR due to more accurate phase estimation [Muthukumaraswamy and Singh, 2011]. This effect can be important for the low-SNR MEG signals whereas SNR of EMG is less critical. However, the observation that CMC was enhanced while rolandic MEG power was still suppressed within the first ~500 ms after auditory distractors speaks for a real physiological phenomenon that cannot be explained by just SNR-related methodological issues.

Mild muscle fatigue was inevitable during the task, despite the low contraction force (~6% of MVC). Previous research has shown that the baseline level of CMC can increase after a fatiguing task [Tecchio et al., 2006a]. In addition, rectification of sEMG prior to coherence analysis can reduce the global level of CMC [McClelland et al., 2012b], although this is not always the case [Yao et al., 2007]. We used unrectifed sEMG. However, in the current study we were interested in the modulation of CMC by distracting stimuli rather than in the global level of CMC. Therefore, the issue of rectification of sEMG, or any time-varying other factors possibly modulating CMC should not affect the current interpretations.

Relation to Action Observation

We have recently shown that 16–20-Hz CMC is phasically enhanced during action observation, starting ~0.5 s after the observed transient finger movement [Hari et al., 2014], at the same time as the rolandic 2–19-Hz MEG power is suppressed. We interpreted these results to imply involvement of at least two neuronal populations in the M1 cortex during action observation: one related to M1 activation and the other related to stabilization of M1 output. In the current study, however, the rolandic MEG power and CMC covaried, as it also happens during own actions [Hari and Salenius, 1999]. It is thus evident that the effects of task-related vs. task-unrelated, or of human vs. nonhuman, visual stimuli on the human M1 cortex can differ. Our current data do not allow a distinction between the underlying mechanisms.

CONCLUSIONS

We found that brief auditory and visual distractors enhance corticospinal coupling during steady isometric contraction and are associated with spatially, temporally, and spectrally similar enhancement of the ~20-Hz mu rhythms. These results indicate that task-unrelated auditory and visual stimuli can influence neuronal circuits responsible for corticospinal coupling. The modulations likely reflect a combination of several mechanisms. We propose that a distractor triggers a covert startle-like response that generates proprioceptive afference to the cortex and the distractor also transiently disengages the subject's attention from the motor task. Consequently, the corticospinal output is readjusted to produce stable contraction force.

ACKNOWLEDGMENT

This study has been supported by the Academy of Finland (grants #131483 and #263800 to Riitta Hari and grant #13266133 to Harri Piitulainen), by the SalWe Research Program for Mind and Body (Tekes — the Finnish Funding Agency for Technology and Innovation grant 1104/10), the European Research Council (Advanced Grant #232946 to Riitta Hari), the Institut d'Encouragement de la Recherche Scientifique et de l'Innovation de Bruxelles (Brussels, Belgium; "Brains Back to Brussels" grant to Veikko Jousmäki), the Fonds de la Recherche Scientifique (FRS-FNRS, Belgium, Research Convention 3.4611.08, Postdoctorate Clinical Master Specialist grant to Xavier De Tiége), and the Helsinki Biomedical Graduate Program of Helsinki University (grant to Eero Smeds).

REFERENCES

Akaike H (1974): A new look at the statistical model identification. IEEE Trans Autom Control 19:716–723.

Alegre M, Labarga A, Gurtubay IG, Iriarte J, Malanda A, Artieda J (2002): Beta electroencephalograph changes during passive movements: Sensory afferences contribute to beta event-related desynchronization in humans. Neurosci Lett 331:29–32.

Aron AR, Poldrack RA (2006): Cortical and subcortical contributions to stop signal response inhibition: Role of the subthalamic nucleus. J Neurosci 26:2424–2433.

Ashburner J, Friston KJ (1999): Nonlinear spatial normalization using basis functions. Hum Brain Mapp 7:254–266.

Ashburner J, Neelin P, Collins DL, Evans A, Friston K (1997): Incorporating prior knowledge into image registration. Neuroimage 6:344–352.

Baker SN (2007): Oscillatory interactions between sensorimotor cortex and the periphery. Curr Opin Neurobiol 17:649–655.

Bortel R, Sovka P (2007): Approximation of statistical distribution of magnitude squared coherence estimated with segment overlapping. Signal Process 87:1100–1117.

Bourguignon M, De Tiège X, Op de Beeck M, Van Bogaert P, Goldman S, Jousmäki V, Hari R (2012a): Primary motor cortex and cerebellum are coupled with the kinematics of observed hand movements. Neuroimage 66C:500–507.

Bourguignon M, Jousmäki V, Op de Beeck M, Van Bogaert P, Goldman S, De Tiège X (2012b): Neuronal network coherent with hand kinematics during fast repetitive hand movements. NeuroImage 59:1684–1691.

Brown P, Salenius S, Rothwell JC, Hari R (1998): Cortical correlate of the Piper rhythm in humans. J Neurophysiol 80:2911–2917.

Caetano G, Jousmäki V, Hari R (2007): Actor's and observer's primary motor cortices stabilize similarly after seen or heard motor actions. Proc Natl Acad Sci USA 104:9058–9062.

Chatrian GE, Petersen MC, Lazarte JA (1959): The blocking of the rolandic wicket rhythm and some central changes related to movement. Electroencephalogr Clin Neurophysiol 11:497–510.

Chen R, Corwell B, Hallett M (1999): Modulation of motor cortex excitability by median nerve and digit stimulation. Exp Brain Res 129:77–86.

Cheyne D, Gaetz W, Garnero L, Lachaux JP, Ducorps A, Schwartz D, Varela FJ (2003): Neuromagnetic imaging of cortical oscillations accompanying tactile stimulation. Brain Res Cogn Brain Res 17:599–611.

Conway BA, Halliday DM, Farmer SF, Shahani U, Maas P, Weir AI, Rosenberg JR (1995): Synchronization between motor cortex and spinal motoneuronal pool during the performance of a maintained motor task in man. J Physiol 489:917–924.

Crawcour S, Bowers A, Harkrider A, Saltuklaroglu T (2009): Mu wave suppression during the perception of meaningless syllables: EEG evidence of motor recruitment. Neuropsychologia 47:2558–2563.

Davis M, Gendelman DS, Tischler MD, Gendelman PM (1982): A primary acoustic startle circuit: Lesion and stimulation studies. J Neurosci 2:791–805.

de Fockert J, Rees G, Frith C, Lavie N (2004): Neural correlates of attentional capture in visual search. J Cogn Neurosci 16:751–759.

Ding M, Bressler SL, Yang W, Liang H (2000): Short-window spectral analysis of cortical event-related potentials by adaptive multivariate autoregressive modeling: Data preprocessing, model validation, and variability assessment. Biol Cybern 83:35–45.

Engel AK, Fries P (2010): Beta-band oscillations–signalling the status quo? Curr Opin Neurobiol 20:156–165.

Faes L, Pinna GD, Porta A, Maestri R, Nollo G (2004): Surrogate data analysis for assessing the significance of the coherence function. IEEE Trans Biomed Eng 51:1156–1166.

Farmer SF, Bremner FD, Halliday DM, Rosenberg JR, Stephens JA (1993): The frequency content of common synaptic inputs to motoneurones studied during voluntary isometric contraction in man. J Physiol 470:127–155.

Gastaut H (1952): Electrocorticographic study of the reactivity of rolandic rhythm (in French). Rev Neurol (Paris) 87:176–182.

Gilbertson T, Lalo E, Doyle L, Di Lazzaro V, Cioni B, Brown P (2005): Existing motor state is favored at the expense of new movement during 13–35 Hz oscillatory synchrony in the human corticospinal system. J Neurosci 25:7771–7779.

Gross J, Tass PA, Salenius S, Hari R, Freund HJ, Schnitzler A (2000): Cortico-muscular synchronization during isometric muscle contraction in humans as revealed by magnetoencephalography. J Physiol 527:623–631.

Gross J, Kujala J, Hämäläinen M, Timmermann L, Schnitzler A, Salmelin R (2001): Dynamic imaging of coherent sources: Studying neural interactions in the human brain. Proc Natl Acad Sci USA 98:694–699.

Halliday DM, Rosenberg JR, Amjad AM, Breeze P, Conway BA, Farmer SF (1995): A framework for the analysis of mixed time series/point process data–theory and application to the study of physiological tremor, single motor unit discharges and electromyograms. Prog Biophys Mol Biol 64: 237–278.

Halliday DM, Conway BA, Farmer SF, Rosenberg JR (1998): Using electroencephalography to study functional coupling between cortical activity and electromyograms during voluntary contractions in humans. Neurosci Lett 241:5–8.

Hari R, Salenius S (1999): Rhythmical corticomotor communication. Neuroreport 10:R1–R10.

Hari R, Forss N, Avikainen S, Kirveskari E, Salenius S, Rizzolatti G (1998): Activation of human primary motor cortex during action observation: A neuromagnetic study. Proc Natl Acad Sci USA 95:15061–15065.

Hari R, Bourguignon M, Piitulainen H, Smeds E, De Tiège X, Jousmäki V (2014): Human primary motor cortex stabilizes during observation of other person's phasic motor actions. Philos Trans B 369:20130171.

Jasper H, Penfield W (1949): Electrocorticograms in man: Effect of voluntary movement upon the electrical activity of the precentral gyrus. Arch Psychiatr Zeitschr Neurol 183:163–174.

Kilner JM, Baker SN, Salenius S, Jousmäki V, Hari R, Lemon RN (1999): Task-dependent modulation of 15–30 Hz coherence between rectified EMGs from human hand and forearm muscles. J Physiol 516:559–570.

Kilner JM, Baker SN, Salenius S, Hari R, Lemon RN (2000): Human cortical muscle coherence is directly related to specific motor parameters. J Neurosci 20:8838–8845.

Kristeva-Feige R, Fritsch C, Timmer J, Lucking CH (2002): Effects of attention and precision of exerted force on beta range EEG-EMG synchronization during a maintained motor contraction task. Clin Neurophysiol 113:124–131.

Kühn AA, Williams D, Kupsch A, Limousin P, Hariz M, Schneider GH, Yarrow K, Brown P (2004): Event-related beta desynchronization in human subthalamic nucleus correlates with motor performance. Brain 127:735–746.

Lepage JF, Tremblay S, Nguyen DK, Champoux F, Lassonde M, Theoret H (2010): Action related sounds induce early and late modulations of motor cortex activity. Neuroreport 21: 250–253.

McClelland VM, Cvetkovic Z, Mills KR (2012a): Modulation of corticomuscular coherence by peripheral stimuli. Exp Brain Res 219:275–292.

McClelland VM, Cvetkovic Z, Mills KR (2012b): Rectification of the EMG is an unnecessary and inappropriate step in the calculation of Corticomuscular coherence. J Neurosci Methods 205:90–201.

Muthukumaraswamy SD, Singh KD (2011): A cautionary note on the interpretation of phase-locking estimates with concurrent changes in power. Clin Neurophysiol 122:2324–2325.

Oldfield RC (1971): The assessment and analysis of handedness: The Edinburgh inventory. Neuropsychologia 9:97–113.

Pfurtscheller G (1992): Event-related synchronization (ERS): An electrophysiological correlate of cortical areas at rest. Electroencephalogr Clin Neurophysiol 83:62–69.

Pfurtscheller G, Neuper C (1997): Motor imagery activates primary sensorimotor area in humans. Neurosci Lett 239:65–68.

Ray NJ, Brittain JS, Holland P, Joundi RA, Stein JF, Aziz TZ, Jenkinson N (2012): The role of the subthalamic nucleus in response inhibition: Evidence from local field potential recordings in the human subthalamic nucleus. Neuroimage 60:271–278.

Riddle CN, Edgley SA, Baker SN (2009): Direct and indirect connections with upper limb motoneurons from the primate reticulospinal tract. J Neurosci 29:4993–4999.

Rizzolatti G, Luppino G, Matelli M (1998): The organization of the cortical motor system: New concepts. Electroencephalogr Clin Neurophysiol 106:283–296.

Rossignol S, Jones GM (1976): Audio-spinal influence in man studied by the H-reflex and its possible role on rhythmic movements synchronized to sound. Electroencephalogr Clin Neurophysiol 41:83–92.

Safri NM, Murayama N, Igasaki T, Hayashida Y (2006): Effects of visual stimulation on cortico-spinal coherence during isometric hand contraction in humans. Int J Psychophysiol 61:288–293.

Safri NM, Murayama N, Hayashida Y, Igasaki T (2007): Effects of concurrent visual tasks on cortico-muscular synchronization in humans. Brain Res 1155:81–92.

Salenius S, Salmelin R, Neuper C, Pfurtscheller G, Hari R (1996): Human cortical 40 Hz rhythm is closely related to EMG rhythmicity. Neurosci Lett 213:75–78.

Salenius S, Portin K, Kajola M, Salmelin R, Hari R (1997a): Cortical control of human motoneuron firing during isometric contraction. J Neurophysiol 77:3401–3405.

Salenius S, Schnitzler A, Salmelin R, Jousmäki V, Hari R (1997b): Modulation of human cortical rolandic rhythms during natural sensorimotor tasks. Neuroimage 5:221–228.

Salmelin R, Hari R (1994): Spatiotemporal characteristics of sensorimotor neuromagnetic rhythms related to thumb movement. Neuroscience 60:537–550.

Salmelin R, Hämäläinen M, Kajola M, Hari R (1995): Functional segregation of movement-related rhythmic activity in the human brain. Neuroimage 2:237–243.

Schelter B, Winterhalder M, Eichler M, Peifer M, Hellwig B, Guschlbauer B, Lucking CH, Dahlhaus R, Timmer J (2006): Testing for directed influences among neural signals using partial directed coherence. J Neurosci Methods 152:210–219.

Schelter B, Timmer J, Eichler M (2009): Assessing the strength of directed influences among neural signals using renormalized partial directed coherence. J Neurosci Methods 179:121–130.

Schneider T, Neumaier A (2001): Algorithm 808: ARfit—A Matlab package for the estimation of parameters and Eigenmodes of multivariate autoregressive models. ACM Trans Math Softw 27:58–65.

Schnitzler A, Salenius S, Salmelin R, Jousmäki V, Hari R (1997): Involvement of primary motor cortex in motor imagery: A neuromagnetic study. Neuroimage 6:201–208.

Sharp DJ, Bonnelle V, De Boissezon X, Beckmann CF, James SG, Patel MC, Mehta MA (2010): Distinct frontal systems for response inhibition, attentional capture, and error processing. Proc Natl Acad Sci USA 107:6106–6111.

Sommerlade L, Eichler M, Jachan M, Henschel K, Timmer J, Schelter B (2009): Estimating causal dependencies in networks of nonlinear stochastic dynamical systems. Phys Rev E Stat Nonlin Soft Matter Phys 80:051128.

Taulu S, Kajola M, Simola J (2004): Suppression of interference and artifacts by the signal space separation method. Brain Topogr 16:269–275.

Tecchio F, Porcaro C, Zappasodi F, Pesenti A, Ercolani M, Rossini PM (2006a): Cortical short-term fatigue effects assessed via rhythmic brain-muscle coherence. Exp Brain Res 174:144–151.

Tecchio F, Zappasodi F, Melgari JM, Porcaro C, Cassetta E, Rossini PM (2006b): Sensory-motor interaction in primary hand cortical areas: A magnetoencephalography assessment. Neuroscience 141:533–542.

Thomson DJ (1982): Spectrum estimation and harmonic analysis. Proc IEEE 70:1055.

Tiihonen J, Kajola M, Hari R (1989): Magnetic mu rhythm in man. Neuroscience 32:793–800.

Vanni S, Portin K, Virsu V, Hari R (1999): Mu rhythm modulation during changes of visual percepts. Neuroscience 91:21–31.

Yao B, Salenius S, Yue GH, Brown RW, Liu JZ (2007): Effects of surface EMG rectification on power and coherence analyses: An EEG and MEG study. J Neurosci Methods 159:215–223.

Yeomans JS, Frankland PW (1995): The acoustic startle reflex: Neurons and connections. Brain Res Brain Res Rev 21:301–314.